Molecular Immunology 63 (2015) 394–405

Contents lists available at ScienceDirect

Molecular Immunology

journal homepage: www.elsevier.com/locate/molimm

The role of poly(ADP-ribose) polymerase-1 inhibitor in carrageenan-induced lung inflammation in mice

Sheikh Fayaz Ahmad[a,*], Khairy M.A. Zoheir[a,b], Mushtaq Ahmad Ansari[a], Hesham M. Korashy[a], Saleh A. Bakheet[a], Abdelkader E. Ashour[a], Othman A. Al-Shabanah[a], Mohammed M. Al-harbi[a], Sabry M. Attia[a,c]

[a] Department of Pharmacology and Toxicology, College of Pharmacy, King Saud University, Riyadh, Saudi Arabia
[b] Department of Cell Biology, National Research Centre, Cairo, Egypt
[c] Department of Pharmacology and Toxicology, College of Pharmacy, Al-Azhar University, Cairo, Egypt

ARTICLE INFO

Article history:
Received 28 May 2014
Received in revised form 7 September 2014
Accepted 17 September 2014
Available online 7 October 2014

Keywords:
Carrageenan
PARP-1 inhibitor
Inflammatory mediators
Pleural exudate
Lung tissue

ABSTRACT

Increasing indication is unveiling a role for poly(ADP-ribose) polymerase (PARP)-1 in the regulation of inflammatory/immune responses. The aim of the present study was to determine the potential anti-inflammatory effects of PARP-1 inhibitor 5-aminoisoquinolinone (5-AIQ) to explore the role of PARP-1 inhibitor in a mouse model of carrageenan-induced lung inflammation. A single dose of 5-AIQ (1.5 mg/kg) was administered intraperitoneally (i.p.) 1 h before λ-carrageenan (Cg) administration. We assessed the effects of 5-AIQ treatment on $CD25^+$, $GITR^+$, $CD25^+GITR^+$, IL-17^+ and $Foxp3^+$ cells which were investigated using flowcytometry in pleural exudates and heparinized blood. We also evaluated mRNA expressions of IL-6, TNF-α, IL-1β, IL-10, CD11a, L-selectin (CD62L), ICAM-1, MCP-1, iNOS and COX-2 in the lung tissue. We further examined the effects of 5-AIQ on the key mediators of inflammation, namely COX-2, STAT-3, NF-kB p65, PARP-1, IkB-α and IL-4 protein expression in the lung tissue using western blotting. The results illustrated that the numbers of T cell subsets, IL-17^+ cytokine levels were markedly increased and $Foxp3^+$ production decreased in the Cg group. Furthermore, Cg-induced up-regulation of adhesion molecules, pro-inflammatory mediators and chemokine expressions. Western blot analysis revealed an increased protein expressions of COX-2, STAT-3 NF-kB p65 and PARP-1 and decreased IkB-α and IL-4 in the Cg group. PARP-1 inhibitor *via* 5-AIQ treatment reverses the action significantly of all the previously mentioned effects. Moreover, histological examinations revealed anti-inflammatory effects of 5-AIQ, whereas Cg-group aggravated Cg-induced inflammation. Present findings demonstrate the potent anti-inflammatory action of the PARP-1 inhibitor in acute lung injury induced by carrageenan.

1. Introduction

The biological significance of poly(ADP-ribose) polymerase (PARP) has been reported in many cellular processes (D'Amours et al., 1999; Shall et al., 2000). Numerous studies have also implicated PARP-1 in the regulation of the inflammatory response (Virag and Szabo, 2002). In this regard, animals treated with PARP-1 inhibitors or PARP-1 deficient mice showed decreased tissue damage and inflammatory mediators in several models of ischemia-reperfusion and heart transplantation (Szabo, 2006). The PARP-1 inhibitor, 5-AIQ, reduces the development of experimental periodontitis in rats, (Paola et al., 2007) as well as ischaemia/reperfusion injury of the heart, intestine, and liver and reduces inflammation and T helper-1 (Th1) responses (Gonzalez-Rey et al., 2007). Furthermore, 5-AIQ treatment shows beneficial effects in rodent models of heart transplantation and colon injury (Szabo et al., 2002; Cuzzocrea et al., 2004). In addition, 5-AIQ also directly inhibits MMP-2 (Nicolescu et al., 2009). Together, these investigations have provided the basis for potential clinical applications of PARP inhibitors.

T lymphocytes are responsible for the initiation and coordination of immune responses and thus play a pivotal role in triggering antigen-specific inflammation. T cell stimulation leads to the up-regulation of several cell surface molecules, including the IL-2R alpha chain, CD25. CD25 expression is not specific to activated T cells; CD25 is also expressed by T regulatory (Tregs) cells and

* Corresponding author. Tel.: +966 569496770.
E-mail addresses: s_fayazahmad@yahoo.com, fashaikh@ksu.edu.sa (S.F. Ahmad).

http://dx.doi.org/10.1016/j.molimm.2014.09.009
0161-5890/

by activated B cells (Sakaguchi et al., 1995). It is well known that glucocorticoid-induced tumour necrosis factor receptor (GITR) plays a co-stimulatory role in effector T cell activation, which is further potentiated by the inhibition of Treg cell function (Nocentini and Riccardi, 2005). Adhesion molecules control the trafficking of leukocytes to the site of the inflammation by means of firm membrane adhesion between leukocytes and the endothelium (Schymeinsky et al., 2007). It is now widely accepted that the production of pro-inflammatory cytokines (TNF-α, IL-1β, and IL-8), the expression of adhesion molecules (intercellular adhesion molecule-1 (ICAM-1)), and the overproduction of vasoactive mediators (nitric oxide (NO)) by inducible NO synthase (iNOS) or eicosanoids by cyclooxygenase-2 (COX-2) by the endothelium and neutrophils each play important roles in the pathophysiology of inflammation (Cuzzocrea et al., 1998).

Multiple studies have demonstrated that nuclear factor-κB (NF-κB) plays a central role in the regulation of many genes responsible for the generation of inflammatory mediators including TNF-α, IL-1, VCAM-1, ICAM-1, and iNOS. Under normal conditions, NF-κB is present within the cytoplasm in an inactive state, bound to the inhibitory protein κB-α (IκB-α). However, inflammatory stimuli initiate an intracellular signalling cascade resulting in phosphorylation of IκB-α on serine residues 32 and 36 by IκB kinase (IKK). Once liberated from its inhibitory protein, NF-κB translocates to the nucleus where it orchestrates the transcription of a number of pro-inflammatory genes (Chen et al., 2000). Additionally, members of the signal transducer and activator of transcription (STAT) family are activated by cytokines during the inflammatory process (Pfitzner et al., 2004). Specifically, cytokines including IL-6, IFN-γ, IL-12, and IL-18, which promote immune and inflammatory responses, use STAT signalling pathways to mediate cellular responses. For example, STAT3 was identified as an acute-phase response factor activated by the pro-inflammatory cytokine IL-6 and by other cytokines that use the gp130 receptor subunit (Levy and Lee, 2002).

Recently, we reported that the PARP-1 inhibitor, 5-aminoisoquinolinone (5-AIQ), modulates Treg and Th17 cell function in the prevention of adjuvant-induced arthritis (Ahmad et al., 2014a). Based upon these results, we hypothesized that PARP-1 inhibition may affect the course of the inflammatory response in a Cg-induced model of acute lung inflammation. In the present study, we explored the effects of 5-AIQ on Cg-induced pleurisy, and examined the underlying mechanisms of 5-AIQ function in this model of acute lung injury. To this end, we investigated the effects of 5-AIQ on $CD25^+$, $GITR^+$, $CD25^+GITR^+$, $IL\text{-}17^+$, and $Foxp3^+$ expressing cells in pleural exudates and in heparinized blood using flow cytometry. We also evaluated IL-6, TNF-α, IL-1β, IL-10, CD11a, L-selectin (CD62L), ICAM-1, MCP-1, iNOS, and COX-2 mRNA expression in lung tissue using RT-PCR. In addition, COX-2, STAT3, NF-κB p65, PARP-1, IκB-α, and IL-4 protein expression in lung tissues were investigated using western blotting and histology.

2. Materials and methods

2.1. Animals

Female adult Balb/c mice, 6–7 weeks old and weighing 20–22 g, were obtained from the Animal Care Center at the College of Pharmacy, King Saud University, Riyadh, Saudi Arabia. The mice were maintained at a room temperature (22 ± 2 °C) with a 12 h light/dark cycle and were housed in a specific pathogen-free environment and fed standard rodent chow and water ad libitum. All procedures were performed with the approval of the Institutional Animal Care and Use Committee.

2.2. Chemicals

5-Aminoisoquinolin (5-AIQ) was obtained from Matrix Scientific (Columbia, USA); Heparin and λ-carrageenan (Cg) were obtained from Sigma-Aldrich (St Louis, USA). Fluoroisothiocyanate (FITC), labelled IL-17, Phycoerythrin (PE), labelled GITR and Foxp3 and Allophycocyanin (APC) labelled CD25 anti-mouse monoclonal antibodies; FcR blocking reagent fixation/Permeabilization and Permeabilization solutions were obtained from Miltenyi Biotech (Bergisch Gladbach, Germany). The primers used in the current study for gene expression were purchased from Applied Biosystems (Paisley, UK) and Genscript (Piscataway, USA). High Capacity cDNA Reverse Transcription kit and SYBR® Green PCR Master Mix were purchased from Applied Biosystems (Paisley, UK). TRIzol were purchased from Life Technologies (Grand Island, USA) Primary and secondary antibodies used for Western blotting were obtained from Santa Cruz (Dallas, USA). Nitrocellulose membrane was purchased from Bio-Rad Laboratories (Hercules, USA). Chemiluminescence Western blot detection kits were obtained from GE Healthcare Life Sciences (Piscataway, USA).

2.3. Experimental design

The mice were acclimatized for seven days and divided randomly into three groups of six mice each. Animals in the first group injected with 0.1 ml normal saline only intraperitoneal (i.p.) and served as control; whereas animals in the second group were injected with 0.1 ml normal saline (NaCl 0.9%) containing Cg (1%) to induce pleurisy and lung inflammation and served as Cg-induced pleurisy; the third group consisted of mice injected with 0.1 ml a single dose of 5-AIQ (1.5 mg/kg, i.p.), 5-AIQ dissolved in double distilled water and was administered one h prior to Cg and served as Cg + 5-AIQ group. The dose of 5-AIQ was selected based on the results of the previous study (Gonzalez-Rey et al., 2007; Ahmad et al., 2014a). The protocol of this study has been approved by Research Ethics Committee of College of Pharmacy, King Saud University (Riyadh, Saudi Arabia).

2.4. Carrageenan-induced pleurisy

Induction of pleurisy by Cg was performed as previously described (Ahmad et al., 2014b. Briefly, mice were injected on the right side of the chest intrapleurally (i.pl.) with 0.1 ml normal saline (NaCl 0.9%) containing Cg (1%). After pleurisy induction (4 h), the animals were anaesthetised by ether, the thorax was opened, and the pleural cavity was washed with 1.0 ml of sterile phosphate buffered saline (PBS).

2.5. Flowcytometry measurement of $CD25^+$, $GITR^+$ and $CD25^+GITR^+$ expressing cells

Pleural exudate was collected from the pleural cavity of all animal groups after light ether was administered as anaesthesia. Monoclonal antibodies conjugated to a fluorochrome and directed against CD25 and GITR were added directly to 100 μl of pleural exudate, which was then lysed using a lysing (Miltenyi Biotech, Bergisch Gladbach, Germany). Following the final wash in PBS, samples were resuspended in PBS (pH 7.4) and analysed directly on the flowcytometer (Beckman Coulter, USA) using CXP software (Ahmad et al., 2014c).

2.6. Measurement of $IL\text{-}17^+$ and $Foxp3^+$ intracellular markers

Heparinized whole blood was collected from the retro-orbital plexus and pleural exudate was collected from the pleural cavity of all animal groups after the administration of light ether as

Table 1
Primer sequences. IL, Interleukin; TNF-α, Tumour necrosis factor-alpha; IL-1β, Interleukin-1 beta; ICAM-1, Intracellular cell adhesion molecule-1; MCP-1, Monocyte chemotactic protein-1; iNOS, Inducible nitric oxide synthase; COX-2, Cyclooxygenase-2; GAPDH, Glyceraldehyde 3-phosphate dehydrogenase.

Gene	Direction and sequence
IL-6	F: 5′-CCGGAGAGGAGACTTCACAG-3′ R: 5′-GGAAATTGGGGTAGGAAGGA-3′
TNF-α	F: 5′-GCGGAGTCCGGGCAGGTCTA-3′ R: 5′-GGGGGCTGGCTCTGTGAGGA-3′
IL-1β	F: 5′-TCGTGCTGTCGGACCCATAT-3′ R: 5′-GTCGTTGCTTGGTTCTCCTTGT-3′
IL-10	F: 5′-ACCTGCTCCACTGCCTTGCT-3′ R: 5′-GGTTGCCAAGCCTTATCGGA-3′
CD11a	F: 5′-AACAAACCCAACGGGACAGT-3′ R: 5′-CTGCAAGCCACTCTACCTCC-3′
CD62L	F: 5′-AAGGTACCGAAGGGATCCGA-3′ R: 5′-GACATGGGTGGGAACCAACA-3′
ICAM-1	F: 5′-GCGGAGTCCGGGCAGGTCTA-3′ R: 5′-GGGGGCTGGCTCTGTGAGGA-3′
MCP-1	F: 5′-ACCACAGTCCATGCCATCAC-3′ R: 5′-TTGAGGTGGTTGTGGAAAAG-3′
iNOS	F: 5′-CTATGGCCGCTTTGATGTGC-3′R: 5′-CAACCTTGGTGTTGAAGGCG-3′
COX-2	F: 5′-CACTCATGAGCAGTCCCCTC-3′ R: 5′-ACCCTGGTCGGTTTGATGTT-3′
GAPDH	F: 5′-CCCAGCAAGGACACTGAGCAAG-3′ R: 5′-GGTCTGGGATGGAAATTGTGAGGG-3′

an anaesthetic. Approximately, 100 μl blood and pleural exudate were pipetted directly into a 12 × 75 mm fluorescence-activated cell sorting (FACS) tube for the assessment of IL-17 and Foxp3 intracellular marker. The RBCs were lysed for 8 min using 3 ml of 1× lysing solution (Miltenyi Biotech, Bergisch Gladbach, Germany). After centrifugation at 300 × *g* for 5 min, the supernatant was aspirated and 1× fixation/permeabilizing solution (500 μl, Miltenyi Biotech) was added into the pellet and incubated for 10 min at room temperature in the dark. The cells were then centrifuged at 300 × *g* for 5 min; the supernatant was aspirated and 1× permeabilizing solution (500 μl) and FcR blocking reagent (10 μl), were added into the pellet and incubated for 10 min at room temperature in the dark. After washing with 3 ml of wash buffer, cytokine-specific antibodies (20 μl) against IL-17 and Foxp3 were added to the cells and incubated for 30 min at room temperature in the dark. Measurements were performed on a flowcytometer (Beckman Coulter, USA). The analysis of the acquired data was accomplished using CXP software application (Ahmad et al., 2014d).

2.7. RNA extraction and cDNA synthesis

All the extraction procedures were performed on ice using ice-cold reagents. Total RNA from the lung tissue homogenate of each mouse was isolated using the TRIzol reagent (Life Technologies, Grand Island, USA) according to the manufacturer's instructions and quantified by measuring the absorbance at 260 nm; the RNA quality was determined by measuring the 260/280 ratio. The cDNA synthesis was performed using the high-capacity cDNA reverse transcription kit (Applied Bio systems, Paisley, UK) according to the manufacturer's instructions and as previously described (Ahmad et al., 2013, 2014e). Briefly, 1.5 μg of total RNA from each sample was added to a mixture of 2.0 μ1 of 10× reverse transcriptase buffer, 0.8 μl of 25× dNTP mix (l00 mM), 2.0 μl of l0× reverse transcriptase random primers, 1.0 μl of multiscribe reverse transcriptase and 3.2 μl of nuclease-free water. The final reaction mixture was held at 25 °C for 10 min, then heated to 37 °C for 120 min and 85 °C for 5 min and, finally, cooled to 4 °C.

2.8. Real-time polymerase chain reaction (RT-PCR) determination of mRNA expressions

Quantitative analysis of the mRNA expression of the target genes was performed by RT-PCR by subjecting the cDNA generated from the above reaction to PCR amplification using 96-well optical reaction plates in the ABI Prism 7500 System (Applied Bio systems, Paisley, UK). The 25 μl reaction mixture included 0.1 μl of the 10 μM forward primer and 0.1 μl of the 10 μM reverse primer (each primer at a final concentration of 40 μM), 12.5 μ1 of the SYBR Green Universal Master mix, 11.05 μ1 of nuclease-free water and 1.25 μ1 of the cDNA sample. The primers used in the current study (Table 1) were chosen from PubMed database (Ansari et al., 2013). The assay controls, namely, the no-template controls, were incorporated onto the same plate to monitor the contamination of assay reagents. The RT-PCR data were analyzed using the relative gene expression (i.e., ΔΔCT) method, as described in the Applied Bio systems User Bulletin No. 2. Briefly, the data are presented as the fold change in gene expression normalized to the endogenous reference gene (GAPDH) and relative to a calibrator.

2.9. Protein extraction and Western blot analysis of COX-2, STAT-3, NF-kB p65, PARP-1, IkB-α and IL-4

The total lung proteins were extracted from lung tissue using previously described method (Barakat et al., 2001). Briefly, lungs were washed in ice cold PBS, cut into small pieces, and homogenized separately in cold protein lysis buffer containing protease inhibitor cocktail (Ansari et al., 2013). Total cellular proteins were obtained by incubating the cell lysates on ice for 1 h, with intermittent vortex mixing every 10 min, followed by centrifugation at 12,000 × g for 10 min at 4 °C. Protein concentrations were measured by Lowry method (Seevaratnam et al., 2009). Western blot analysis was performed using a previously described method (Sambrook et al., 1989). Briefly, 25–50 μg of protein from each group was separated by 10% SDS-polyacrylamide gel electrophoresis (PAGE) and electrophoretically transferred in to nitrocellulose membrane (Bio-Rad, USA). Protein blots were blocked overnight at 4 °C, followed by incubations with a primary antibodies against COX-2, STAT-3, NF-kB p65, PARP-1, IkB-α and IL-4 (Santa Cruz, Dallas, USA), followed by incubation for 2 h with peroxidase-conjugated secondary antibodies at room temperature. The COX-2, STAT-3, NF-kB p65, PARP-1, IkB-α and IL-4 bands were visualized using the enhanced chemiluminescence method (GE Health care, Mississauga, Canada) and quantified relative to β-actin bands using ImageJ®, image processing program (National Institutes of Health, Bethesda, USA). Images were taken on C-Digit chemiluminescent Western blot scanner (LI-COR, Lincoln, USA).

2.10. Malondialdehyde measurement

Malondialdehyde (MDA) levels in the lung tissue were determined as an indicator of lipid peroxidation as described previously (Impellizzeri et al., 2011). Lung tissue collected at the specified time was homogenized in 1.15% (w/v) KCl solution. A 100 μl aliquot of the homogenate was added to a reaction mixture containing 200 μl of 8.1% (w/v) SDS, 1.5 ml of 20% (v/v) acetic acid (pH 3.5), 1.5 ml of 0.8% (w/v) thiobarbituric acid and 700 μl distilled water. Samples were boiled for 1 h at 95 °C using glass ball as condensers. After cooling under tap water, samples were centrifuged at 4000 × *g* for 10 min and the absorbance of the supernatant was measured using spectrophotometer at 650 nm against a blank.

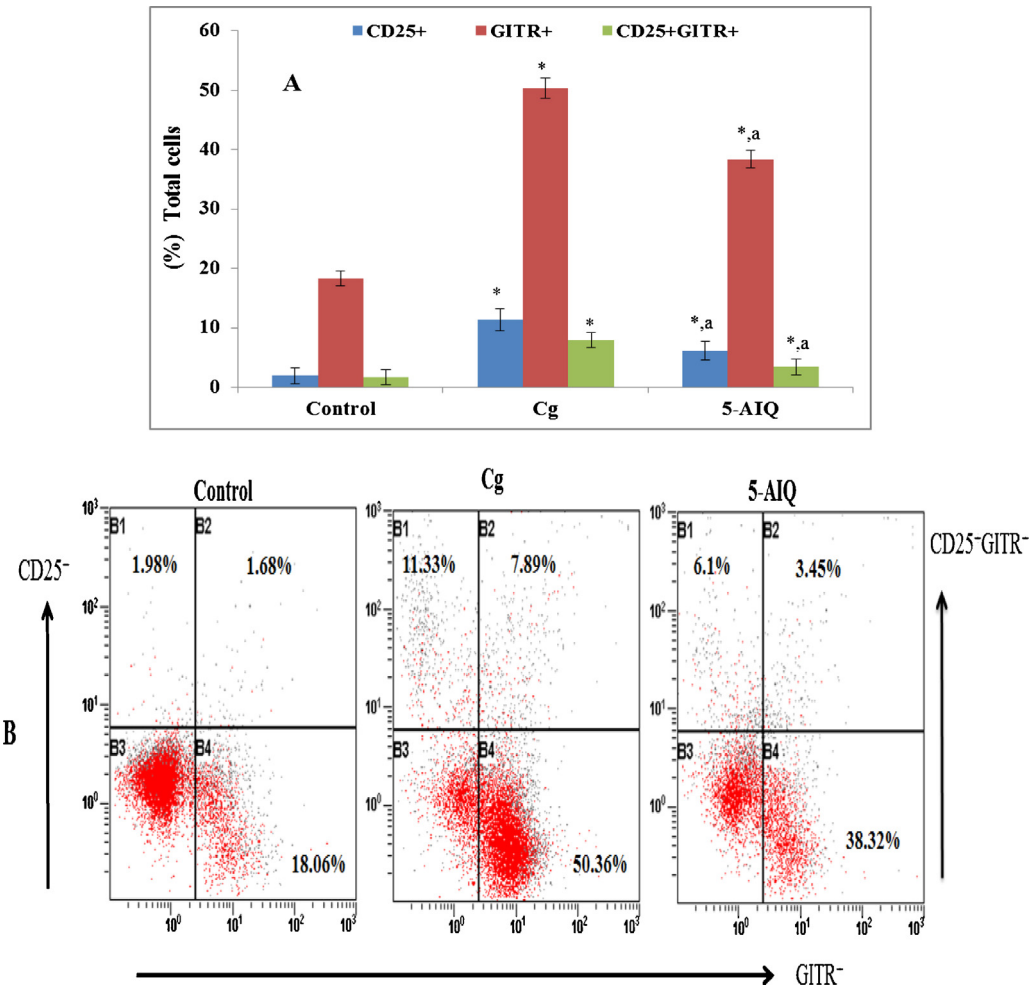

Fig. 1. (A) Effect of 5-AIQ on $CD25^+$, $GITR^+$ and $CD25^+GITR^+$ populations in pleural exudate. Flow cytometric analysis of GITR and CD25 expression on pleural exudate cells at 4 h after the induction of pleurisy *via* Cg injection. Statistical analysis was performed using a one-way ANOVA followed by the Tukey–Kramer post-test. Each value indicates the mean ± S.E.M of six animals. $p < 0.05$ was considered significant; (*) compared to the control group; (a) compared to the Cg control group. (B) Representative dot plots are shown for $CD25^+$, $GITR^+$ and $CD25^+GITR^+$ expressing cells in the pleural exudate cells from one mouse from each group at 4 h.

2.11. Histological examination of the lung tissue

Lung tissue samples isolated from all groups were fixed for 1 week in buffered formaldehyde solution (10% in PBS) at room temperature, dehydrated by graded ethanol and embedded in Paraplast (Sherwood Medical, Mahwah, NJ). Tissue sections (thickness 7 μm) were deparaffinised with xylene stained with hematoxylin and eosin (H&E) stains and then studied using light microscopy (Olympus, USA). All the histological studies were performed in a blinded fashion on a 0–10 scale to avoid scoring biases (Ahmad et al., 2014b). The following morphological criteria were used for scoring: 0, normal lung; grade 3, minimal oedema or infiltration of alveolar or bronchiolar walls; grade 5, inflammatory cell infiltration with lobar lung pneumonia, alveolar septum and occasional obliterated alveoli with obvious damage to lung architecture; grade 7, severe inflammatory cell infiltration with obvious damage to lung architecture.

2.12. Data analysis

All values in the figures and the text are expressed as the mean ± standard error of the mean (S.E.M.). The differences between treatment groups were analyzed by one way analysis of variance (ANOVA) followed by a Tukey–Kramer test for comparisons between groups. A value of $^* p < 0.05$ was considered statistically significant.

3. Results

3.1. Effect of 5-AIQ on $CD25^+$, $GITR^+$, and $CD25^+GITR^+$ expressing cells

Flowcytometric analyses of pleural exudate cells revealed a substantial increase in $CD25^+$, $GITR^+$, and $CD25^+GITR^+$ expressing cell subsets in mice four hours post-Cg injection as compared to untreated control mice (Fig. 1A and B). Strikingly, pre-treatment of Cg-injected animals with 5-AIQ significantly reduced $CD25^+$, $GITR^+$, and $CD25^+GITR^+$ expressing cell subsets (Fig. 1 A and B). Together, these data indicate that inhibition of PARP-1 reduces the recruitment of inflammatory cells during Cg-induced pleurisy.

3.2. Effect of 5-AIQ on $IL\text{-}17^+$ production and $Foxp3^+$ Treg cell recruitment

Injection of mice with a single dose of Cg significantly increased the proportion of $IL\text{-}17^+$ cells with a concomitant decrease in the percentage of cells expressing $Foxp3^+$ as compared to untreated control mice (Fig. 2A and B). Importantly, treatment of mice with 5-AIQ prior to injection with Cg resulted in a marked reduction

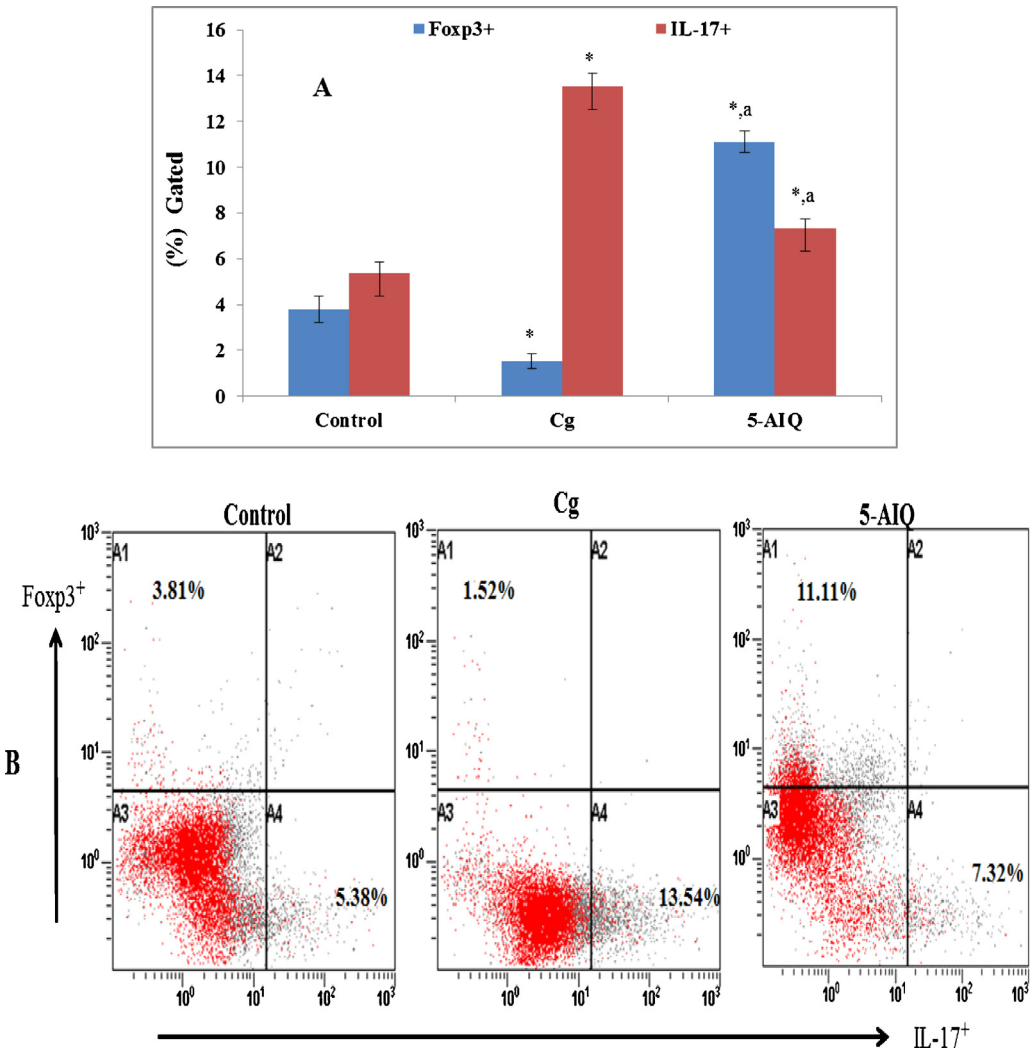

Fig. 2. (A) Effect of 5-AIQ on IL-17$^+$ and Foxp3$^+$ expression in whole blood. Flow cytometric analysis of whole blood at 4 h after the induction of pleurisy *via* Cg injection. Statistical analysis was performed using a one-way ANOVA followed by the Tukey–Kramer post-test. Each value indicates the mean ± S.E.M of six animals. $p < 0.05$ is accepted as the level of significance; (*) compared to the control group; (a) compared to the Cg control group. (B) Representative dot plots are shown for IL-17$^+$ and Foxp3 staining in whole blood from one mouse from each group at 4 h.

in the total percentage of IL-17$^+$ cells, which was accompanied by an increased proportion of Foxp3$^+$ expressing cells as compared to treatment of mice with Cg alone (Fig. 2A and B) in the whole blood.

An increase in the production of IL-17$^+$ in the pleural exudate of animals following the induction of Cg-induced pleurisy was observed compared to the untreated control mice. 5-AIQ significantly decreased IL-17$^+$ cells cytokine level. Administration of Cg alone (to induce pleurisy) resulted in a significant decrease in Foxp3$^+$ production compared to the untreated control mice. Treatment with 5-AIQ increased Foxp3$^+$ cytokine production compared to Cg-treated mice, and the production was considerably greater than that of the untreated control mice (Fig. 3A and B). Together, these data suggest that inhibition of PARP-1 contributes to decreased inflammation by reducing recruitment of IL-17$^+$ cells and by increasing the proportion of Foxp3$^+$ Treg cells in the lungs following Cg treatment.

3.3. Effect of 5-AIQ on IL-6, TNF-α, IL-1β, and IL-10 mRNA expression

We further characterized the effect of 5-AIQ in Cg-induced lung inflammation by measuring mRNA levels of pro-inflammatory (IL-6, TNF-α, and IL-1β) and anti-inflammatory (IL-10) mediators in the lung tissue of Cg-treated mice four hours post-injection. Our results showed that induction of lung inflammation by Cg significantly increased the levels of IL-6, TNF-α, and IL-1β mRNA (Fig. 4A–C), whereas it significantly decreased the levels of IL-10 mRNA as compared to mice in the control group (Fig. 4D). In contrast, as compared to mice treated with Cg only, pre-treatment of Cg injected mice with 5-AIQ resulted in a marked decrease in the mRNA levels of pro-inflammatory cytokines and an increase in message expression for the anti-inflammatory cytokine, IL-10.

3.4. Effect of 5-AIQ on CD11a, CD62L, ICAM-1, and MCP-1 mRNA expression

We further examined the anti-inflammatory effect of PARP-1 inhibition by 5-AIQ in Cg-injected mice by measuring mRNA expression of the cell adhesion molecules and chemokines, CD11a, CD62L, ICAM-1, and MCP-1. In this regard, a substantial increase in CD11a, L-selectin (CD62L), ICAM-1, and MCP-1 mRNA levels was observed in the lung tissue isolated from Cg-treated mice *versus* untreated, control mice (Fig. 5A–D). Acute administration of 5-AIQ prior to induction of lung pleurisy by Cg resulted in a significant

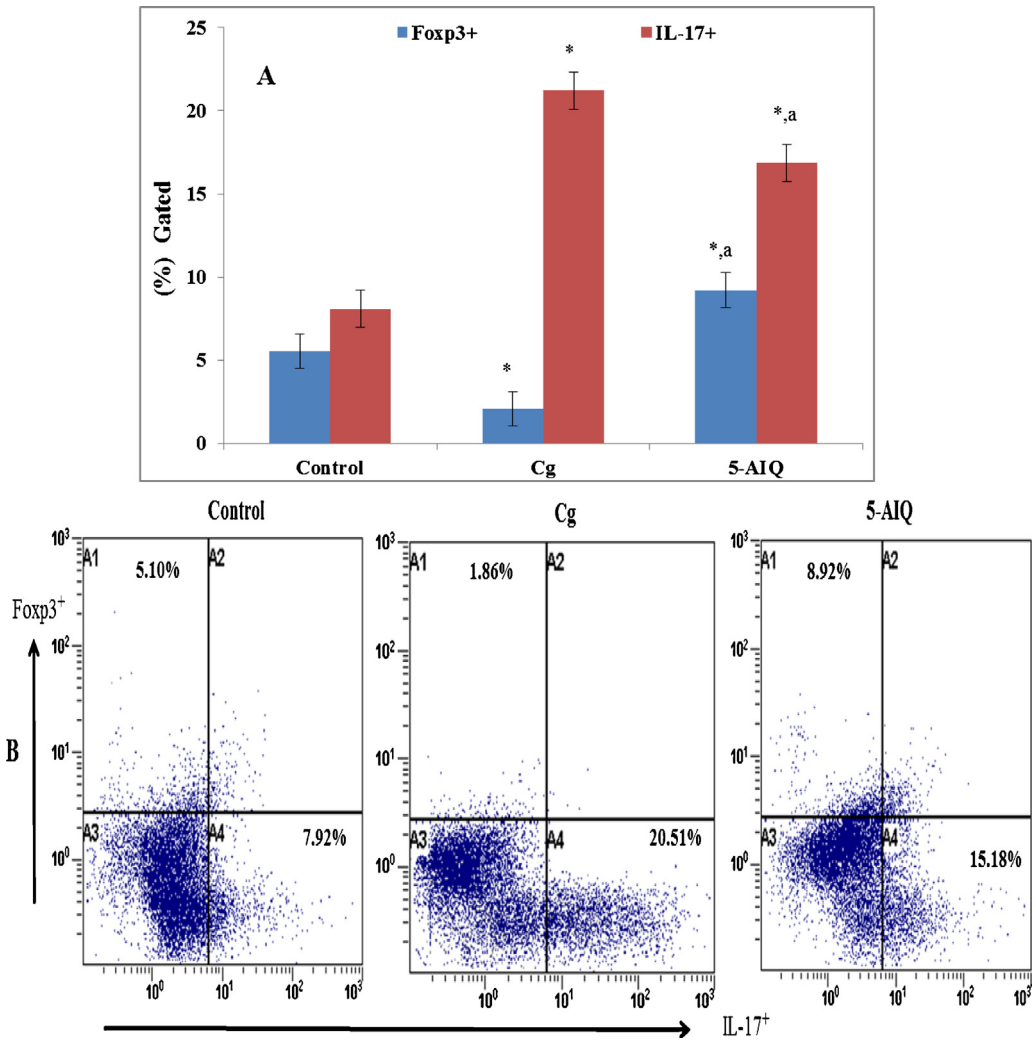

Fig. 3. (A) Effect of 5-AIQ on IL-17$^+$ and Foxp3$^+$ expression in pleural exudate. Flow cytometric analysis of pleural exudate at 4 h after the induction of pleurisy *via* Cg injection. Statistical analysis was performed using a one-way ANOVA followed by the Tukey–Kramer post-test. Each value indicates the mean ± S.E.M of six animals. $p < 0.05$ is accepted as the level of significance; (*) compared to the control group; (a) compared to the Cg control group. (B) Representative dot plots are shown for IL-17$^+$ and Foxp3$^+$ staining in pleural exudate from one mouse from each group at 4 h.

reduction in CD11a, CD62L, ICAM-1, and MCP-1 mRNA levels as compared to mice in the Cg treated group (Fig. 5).

3.5. Effect of 5-AIQ on iNOS and COX-2 mRNA expression

We further characterized the effect of 5-AIQ treatment on Cg-induced inflammation by measuring iNOS and COX-2 mRNA levels in untreated control mice, Cg-injected mice, and Cg-injected mice pre-treated with 5-AIQ. These experiments showed that Cg-induced lung inflammation was associated with a significant induction in the mRNA expression of both iNOS and COX-2 in the lung tissue, as compared to control group (Fig. 6A and B). Strikingly, pre-treatment with 5-AIQ significantly reversed the changes in expression of both iNOS and COX-2 mRNAs (Fig. 6) further supporting an anti-inflammatory role for PARP-1 inhibition in lung inflammation induced by Cg.

3.6. Effect of 5-AIQ treatment on lipid peroxidation

Malondialdehyde (MDA) is a biomarker of lipid peroxidation that is associated with tissue injury and inflammation. Thus, we measured levels of MDA in the lung tissue from untreated control mice, Cg-injected mice, and Cg-injected mice pre-treated with 5-AIQ. As shown in Fig. 6, injection of mice with Cg resulted in a 4-fold increase in MDA as compared to mice in the control group. In contrast, pre-treatment of Cg-injected mice with 5-AIQ resulted in a significant reduction in lung MDA levels (Fig. 7). Thus, not only does 5-AIQ treatment reduce the recruitment of pro-inflammatory cells to lungs and the production of pro-inflammatory mediators, but it also results in a reduction in the overall inflammation and tissue injury that results from Cg treatment.

3.7. Effect of 5-AIQ on NF-κB p65, IκB-α, STAT3, COX-2, IL-4 and PARP-1 protein expression

We studied the effects of 5-AIQ on protein expression of NF-κB p65. Western blotting analyses of lysates generated from lung tissue isolated from untreated control mice, Cg-injected mice, and Cg-injected mice pre-treated with 5-AIQ revealed that the Cg-treated group had significantly increased NF-κB p65 protein expression with a sharp decrease in IκB-α as compared to the control group. Importantly, treatment of mice with 5-AIQ significantly prevented the activation of NF-κB p65 and the degradation of IκB-α. Similarly, STAT3 expression was significantly elevated four hours

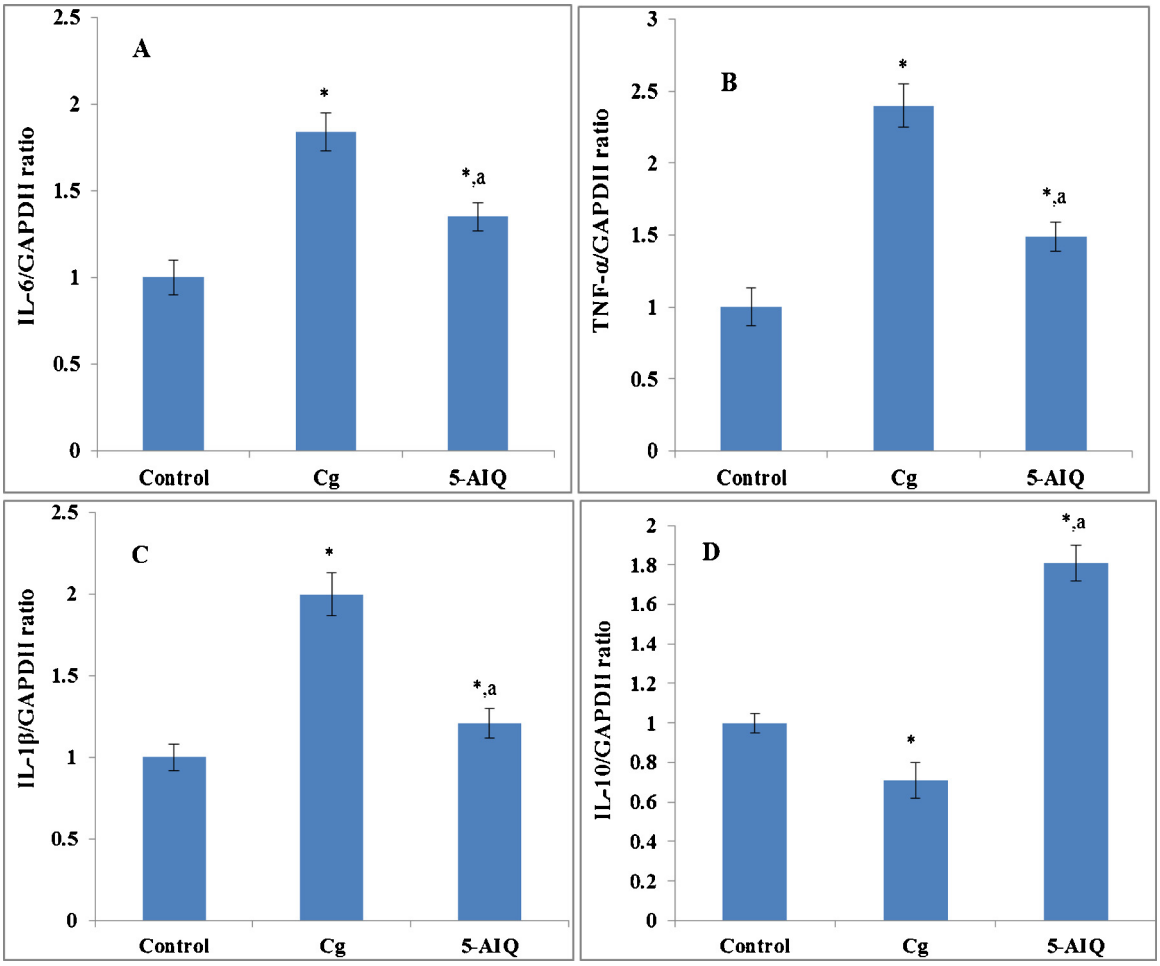

Fig. 4. Effect of 5-AIQ on the gene expression of pro- and anti-inflammatory (A) IL-6, (B) TNF-α, (C) IL-1β and (D) IL-10 cytokines. mRNA expression was measured by quantitative RT-PCR in the lung tissue at 4 h after the induction of pleurisy by Cg injection. Statistical analysis was performed using a one-way ANOVA followed by the Tukey–Kramer post-test. Each value indicates the mean ± S.E.M of six animals. $p < 0.05$ was considered significant; (*) compared to the control group; (a) compared to the Cg control group.

after Cg administration and was markedly reduced by 5-AIQ treatment as compared to Cg-treated group (Fig. 8A).

In contrast to lung tissue isolated from mice in the control group, a significant increase in COX-2 protein levels was detected in lung tissue isolated from mice in the Cg-injected group. Strikingly, pre-treatment with 5-AIQ significantly reduced Cg-induced expression of COX-2. Furthermore, Cg-injected mice showed reduced IL-4 protein expression as compared to untreated mice, while it was elevated in 5-AIQ treated mice as compared to Cg-injected mice. Statistically significant decrease of PARP-1 protein expression was determined in mice treated with 5-AIQ (Fig. 8B).

3.8. Effect of 5-AIQ on lung inflammation

Histological examination of lung tissue revealed that lung sections from the untreated, control group contained healthy, patent alveoli (Fig. 9). In contrast, lungs from Cg-injected mice showed dense inflammation with lobar lung pneumonia and thickened alveolar lung septum with occasionally obliterated alveoli (Fig. 9). Pre-treatment of Cg-injected mice with 5-AIQ induced a protective effect. In this regard, 5-AIQ treatment on Cg-injected animals resulted in reduced inflammation and inflammatory cell infiltration, an increase in patent areas of the lung alveoli, and overall healthier looking areas with a few congestive stage patches (Fig. 9).

4. Discussion

Injection of carrageenan into the pleural cavity of animals induces an acute inflammatory response characterized by increased pleural cavity fluid containing a large number of polymorphonuclear leukocytes (PMN). In addition, there is infiltration by these cells into lung tissue leading to lipid peroxidation and increased production of prostaglandin E2, reactive oxygen intermediates, and inflammatory cytokines (Paul et al., 2009). Moreover, as shown earlier and presently confirmed, Cg also upregulates expression of adhesion molecules, *P*-selectin, chemokines, and cytokines (Katz et al., 2001; Cuzzocrea et al., 2002).

Poly(ADP-ribosylation) has been implicated in many processes such as DNA replication, repair, and transcription (Hakme et al., 2008). Its active involvement in gene expression and chromatin organization has also been demonstrated (Kraus, 2008). PARP-1 over-activation mediated by the generation of free radicals, reactive oxygen species, and peroxynitrite can be detrimental because of energy depletion and consequent necrosis of neuronal cells, immune-stimulated macrophages, endothelial cells, and fibroblasts (Esposito and Cuzzocrea, 2009).

The PARP-1 inhibitor, 5-AIQ, exerts a protective effect countering a number of inflammatory conditions (Hendryk et al., 2008). Specifically, 5-AIQ have been shown to attenuate inflammation

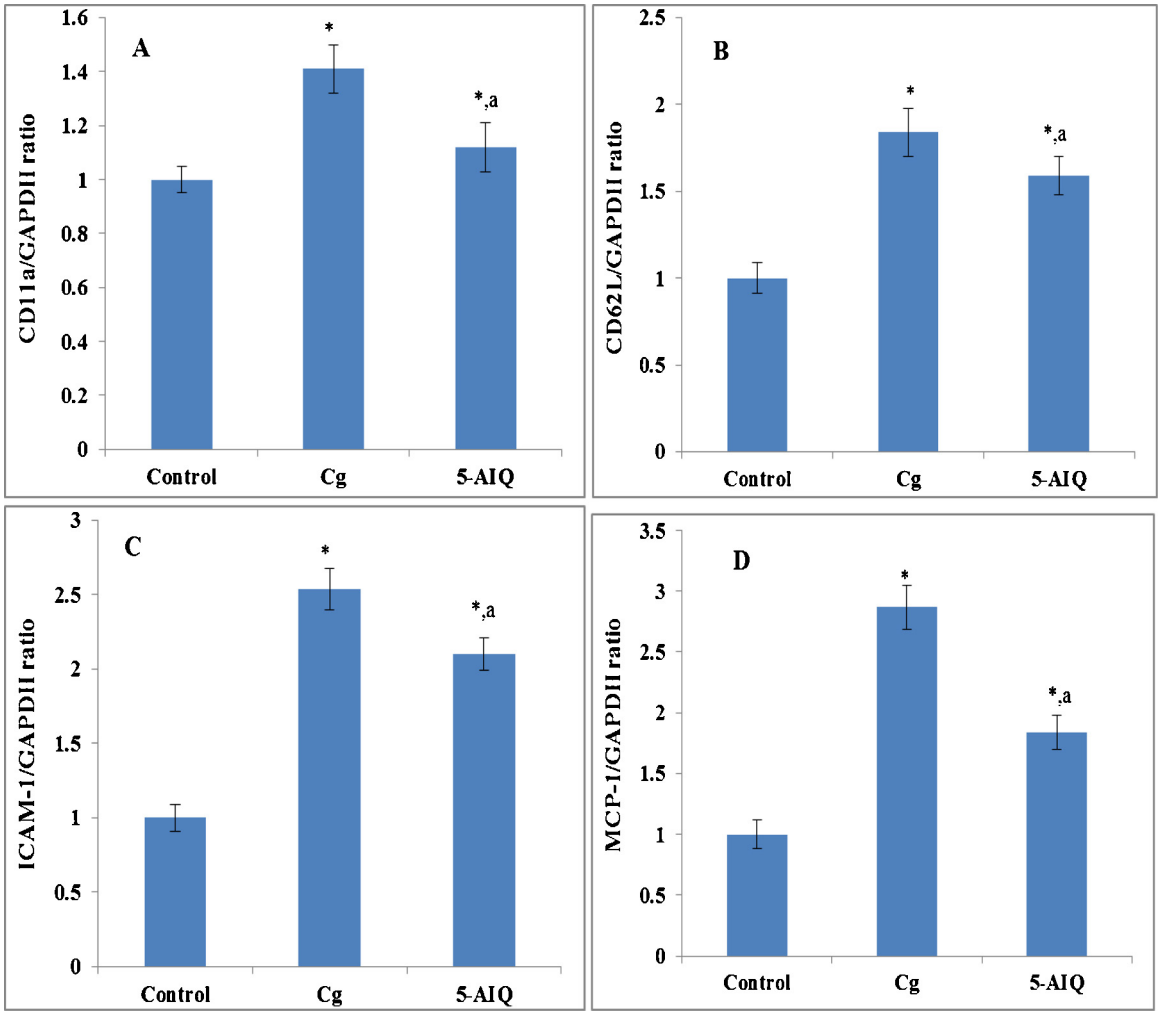

Fig. 5. Effect of 5-AIQ on the gene expression of cell adhesion molecules (A) CD11a, (B) CD62L, (C) ICAM-1, and (D) MCP-1 mediators. mRNA expression was measured by quantitative RT-PCR in the lung tissue at 4 h after the induction of pleurisy by Cg injection. Statistical analysis was performed using a one-way ANOVA followed by the Tukey–Kramer post-test. Each value indicates the mean ± S.E.M of six animals. $p < 0.05$ was considered significant; (*) compared to the control group; (a) compared to the Cg control group.

and rescue animals from many pathological processes (Paola et al., 2007; Pacher and Szabo, 2007). Recently, certain inhibitors of poly(ADP-ribose) synthase activation have been described as potent anti-inflammatory drugs with therapeutic efficacy in experimental models of inflammation such as arthritis, pleurisy, and paw oedema, and in ischemia and reperfusion injury of myocardium and splanchnic tissue (Zingarelli et al., 1998; Ahmad et al., 2014e).

In the present study, we evaluated the protective role of 5-AIQ in Cg-induced lung inflammation. Initially, induction of lung inflammation by Cg was evidenced by (a) increased recruitment of T cell subsets into, and IL-17 in, pleural exudate, and (b) increased mRNA expression of several pro-inflammatory mediators in lung tissue. Importantly, pre-treatment with 5-AIQ markedly reversed all changes induced by Cg, supporting the notion that inhibition of

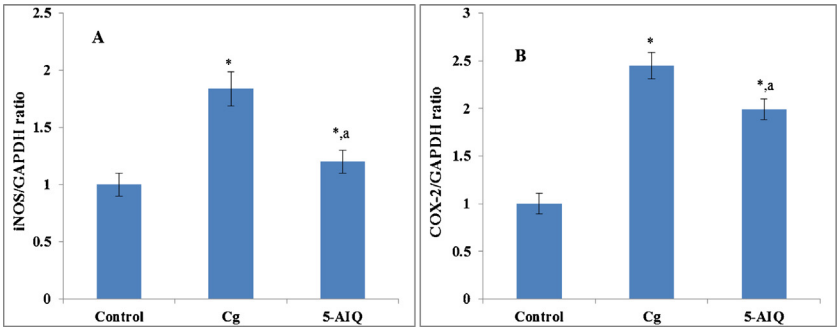

Fig. 6. Effect of 5-AIQ on the gene expression of (A) iNOS and (B) COX-2 activation. mRNA expression was measured by quantitative RT-PCR in the lung tissue at 4 h after the induction of pleurisy by Cg injection. Statistical analysis was performed using a one-way ANOVA followed by the Tukey–Kramer post-test. Each value indicates the mean ± S.E.M of six animals. $p < 0.05$ was considered significant; (*) compared to the control group; (a) compared to the Cg control group.

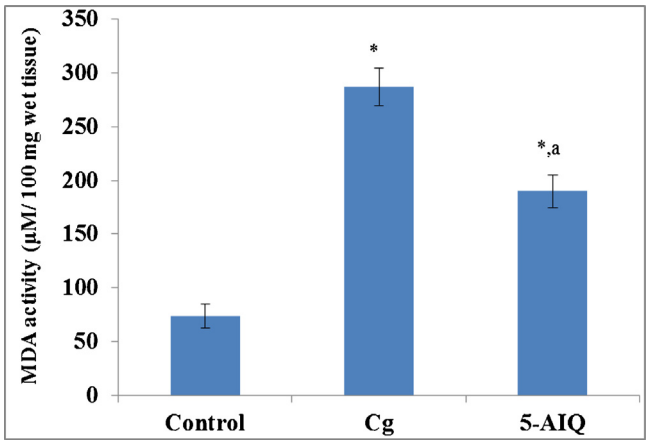

Fig. 7. Effect of 5-AIQ on MDA levels in the lung tissue at 4 h after the induction of pleurisy by Cg injection. Statistical analysis was performed using a one-way ANOVA followed by the Tukey–Kramer post-test. Each value indicates the mean ± S.E.M of six animals. $p < 0.05$ was considered significant (*) compared to the control group; (a) compared to the Cg control group.

PARP-1 inhibitor possess results in anti-inflammatory effects and has potential therapeutic application for the treatment of inflammatory diseases.

The protective effect and mechanism of action of 5-AIQ against Cg-induced lung inflammation is supported by the following observations. First, 5-AIQ potently inhibits the recruitment of T cell subsets and GITR expressing cells into the plueral cavity. In addition to being expressed by T lymphocytes, GITR is expressed on several cell types that participate in the inflammatory response. In particular, GITR is expressed on PMN and macrophages (Nocentini and Riccardi, 2005; Ko et al., 2005). It is well known that GITR plays a co-stimulatory function during effector T cell activation, further potentiated by the inhibition of Treg cell function upon its triggering (Nocentini and Riccardi, 2005).

Second, 5-AIQ treatment decreased the production of IL-17$^+$ and increased recruitment of Foxp3$^+$ cells into the pleural cavity that results from Cg treatment. In this regard, IL-17 is known to play a pivotal role in the inflammatory process *via* stimulation of the synthesis of other pro-inflammatory cytokines, such as TNF-α, IL-1β, IL-6, and prostaglandins (Hurst et al., 2002). Furthermore, T cells expressing the transcription factor Foxp3 play a key role in the immune system apparatus that controls inflammatory processes (Hori et al., 2003). Our results clearly suggest that the anti-inflammatory action of 5-AIQ in a mouse model of pleurisy can be, in part, attributed to the reduction of IL-17 production concomitant with an increase in Foxp3$^+$ T cells at the site of lung inflammation.

Third, activation and release of pro-inflammatory cytokines, such as IL-6, TNF-α, IL-1β, and IFN-γ by pleural mesothelial cells in response to Cg allows cell influx into the pleural cavity (Oliveira et al., 2008) and stimulates cellular chemotaxis and the expression of the adhesion molecules (Borish and Steinke, 2003) As a

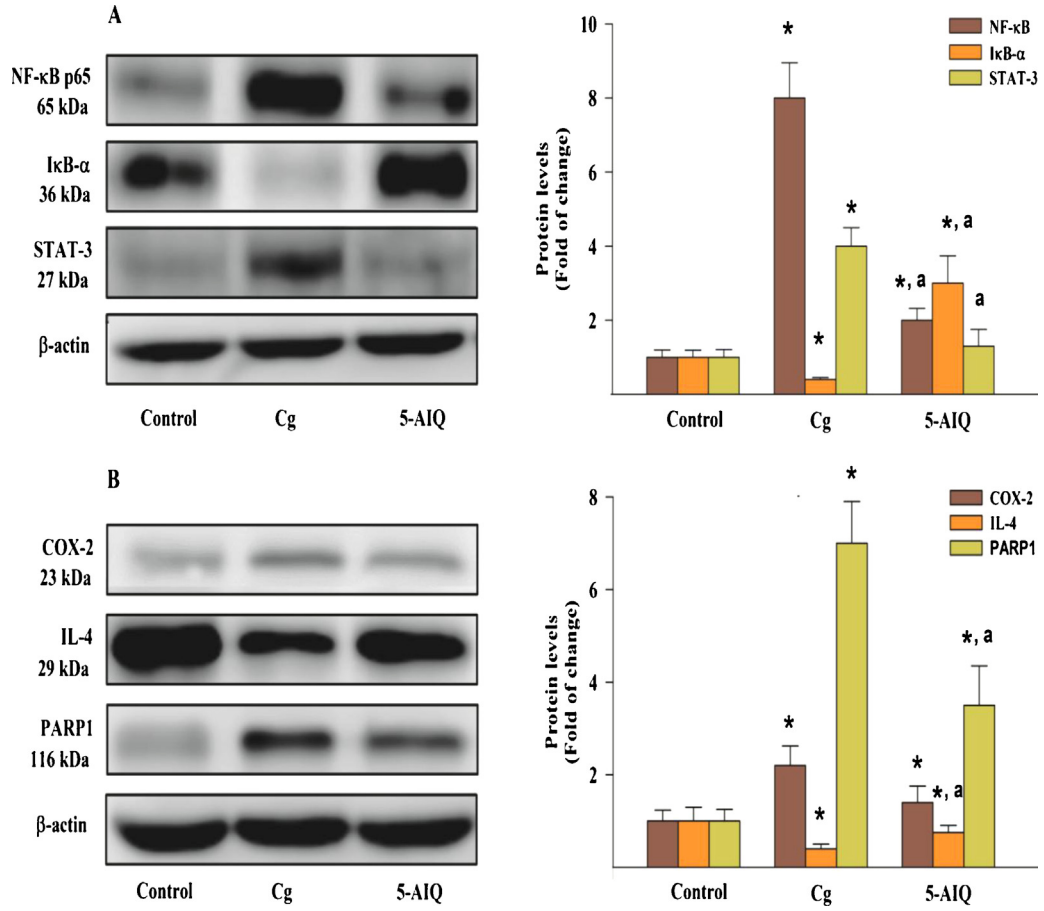

Fig. 8. Effect of 5-AIQ on the activation of (A) NF-kB p65, IkB-α and STAT-3 (B) COX-2, IL-4 and PARP-1. Protein expression was detected by western blots analysis in the lung tissues at 4 h after the induction of pleurisy by Cg injection. Statistical analysis was performed using a one-way ANOVA followed by the Tukey–Kramer post-test. Each value indicates the mean ± S.E.M of six animals. $p < 0.05$ was considered significant; (*) compared to the control group; (a) compared to the Cg control group.

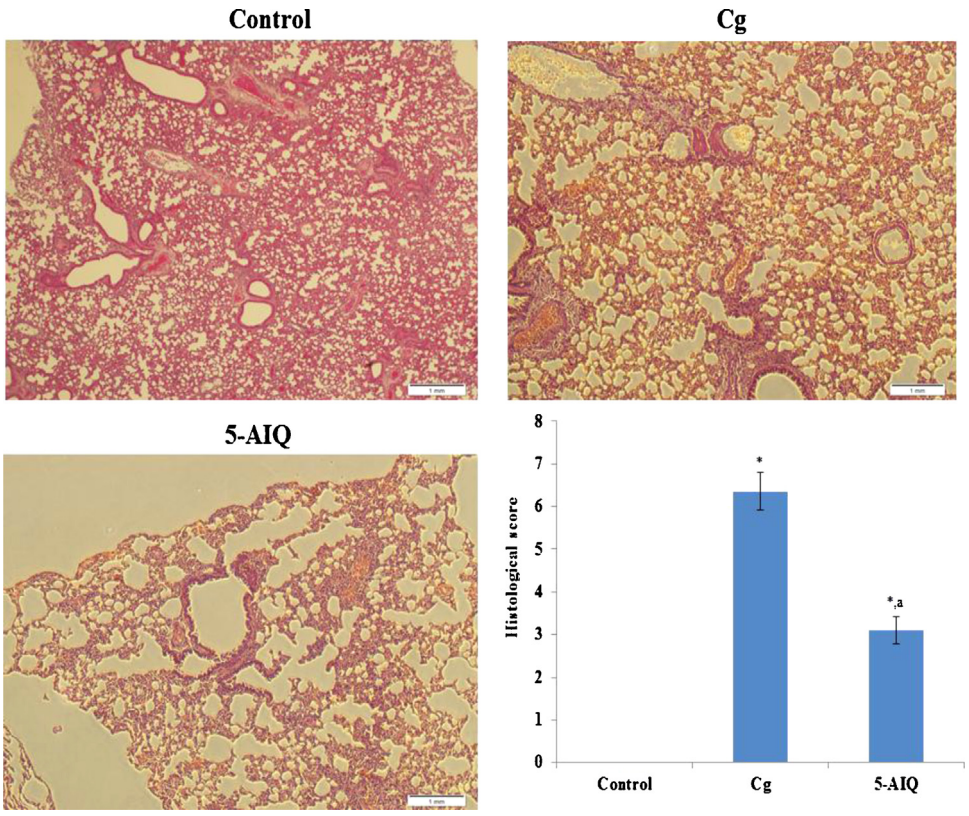

Fig. 9. The effect of 5-AIQ on lung histology following 4 h of Cg administration in a mouse pleurisy model. Histological scoring was conducted by an independent observer. Statistical analysis was performed using a one-way ANOVA followed by the Tukey–Kramer post-test. Each value indicates the mean ± S.E.M of six animals. $p < 0.05$ was considered signficant; (*) compared to the control group; (a) compared to the Cg control group.

compensatory response, the body produces the anti-inflammatory cytokine, IL-10 (Lina et al., 2008). Our results demonstrate that treatment with 5-AIQ significantly inhibits the production of mRNA for several pro-inflammatory cytokines following Cg-injection.

Fourth, attenuation of the Cg-mediated induction of mRNA expression of several adhesion molecules including CD11a, CD62L, ICAM-1, and MCP-1 by 5-AIQ is another postulated mechanism of action of 5-AIQ treatment. CD11a is expressed in neutrophils, monocytes, macrophages, and other cells (Nishibori et al., 2003; Kirchberger et al., 2006). L-selectin (CD62L) is an adhesion molecule expressed on most leukocytes that is involved in the recruitment of these cells to sites of inflammation, an effect that was originally shown by reduced leukocyte migration into inflamed skin in mice treated with the L-selectin blocking mAb, MEL-14 (Lewinsohn et al., 1987). The level of ICAM-1 expression on the surface of any given cell type depends upon the concentrations of pro- and anti-inflammatory mediators and on the availability of specific receptor-mediated signal transduction pathways and their nuclear transcription factor targets in the ICAM-1 promoter (Cornelius et al., 1993). The major intracellular signal transduction pathways involved in the regulation of ICAM-1 expression include protein kinase C (PKC), the mitogen-activated protein (MAP) kinases, and the NF-κB signalling pathway (Ballestas and Benveniste, 1995; Tamura et al., 1998). In addition, the monocyte chemo-attractant protein-1 (MCP-1) is known to be important for neutrophil recruitment (Christopherson and Hromas, 2001). Thus, regulation of the expression of these adhesion molecules affects multiple immune pathways.

Fifth, the ability of 5-AIQ to attenuate Cg-induced oxidative stress markers is another hypothesized mechanism by which it reduces Cg-induced lung disease and is supported by the following observations. First, 5-AIQ significantly inhibited the expression of iNOS, which is known to mediate the production of pro-inflammatory nitric oxide (NO) associated with the initiation and maintenance of different experimental and clinic pathologies including lung disease. Overproduction of NO leads to oxidative stress is one cause of cell death and tissue damage that characterizes a number of pathologies (Hesslinger et al., 2009; May et al., 2009). Second, 5-AIQ treatment downregulated levels of COX-2 mRNA, a protein shown to increase levels of a central mediator of inflammation, PGE2 (Sun et al., 2010). Finally, 5-AIQ reduced MDA and lipid peroxidation levels in Cg-inflamed lung tissue.

It has been reported that PARP-1 physically interacts with NF-κB, one of the main pro-inflammatory transcription factors (Karin. and Delhase, 1998). The NF-κB pathway is a therapeutic target in inflammatory diseases due to the important role of this molecule in the transcriptional activation of TNF-α, IL-1β, COX-2, IL-2, IL-6, IL-8, and iNOS expression (Zhou et al., 2008; Farombi et al., 2009). Inappropriate regulation of NF-κB is directly involved in a wide range of human disorders, neurodegenerative diseases, arthritis, inflammatory bowel disease and numerous other inflammatory conditions. Thus, agents that inhibit NF-κB activation have anti-inflammatory effects (Moon et al., 2009). In this study, we confirmed that Cg injection produced a substantial increase in NF-κB p65 and PARP-1 protein expression in the lung tissue, whereas 5-AIQ treatment significantly reduced the NF-κB p65 and PARP-1 protein expression. Recent studies have indicated that STAT3 is activated in the lung following acute lung injury, (Gao et al., 2004) and STAT3 is known to be a central regulator of lymphocyte differentiation and function (Kane et al., 2014). For example, STAT3 regulates cytokine-mediated generation of inflammatory Th17 cells (Renner et al., 2008). The present study demonstrated that 5-AIQ diminishes STAT3 expression in the lung tissue from Cg-treated mice.

To further clarify the mechanism of the action of 5-AIQ, we examined protein expression of IL-4 in the lung tissue by western blot analysis. The expression of the anti-inflammatory cytokine IL-4 was significantly decreased in the presence of Cg, whereas treatment with 5-AIQ significantly increased protein expression of IL-4 as compared to Cg treated animals. Moreover, a significant down-regulation in the protein expression of IL-4 was still observed in 5-AIQ treated animals as compared to normal control mice (untreated mice). These observations are in line with earlier reports (Gonzalez-Rey et al., 2007; Olabisi et al., 2008; Saenz et al., 2008). IL-4 plays a central role in regulating the differentiation of antigen-stimulated naive T-cells into Th2 cells that produce anti-inflammatory cytokines (Seder et al., 1992) and is responsible for suppressing the synthesis of pro-inflammatory cytokines by macrophages and monocytes.

5. Conclusions

Our current study demonstrated that treatment of mice with 5-AIQ effectively controls the inflammatory response induced by Cg injection. Animals treated with 5-AIQ not only attenuated T cell subsets, but also the production of pro-inflammatory mediators following Cg administration. Thus, this allowed for the accelerated reduction of inflammation and the prevention of the infiltration of inflammatory cells into the damaged tissue through the downregulation of inflammatory mediators. The results of this study deliver a complete assessment of the immunosuppressive pathways by which the 5-AIQ regimen induces a potent protective effect against Cg-induced pleurisy.

Conflict of interest statement

The authors declare that there is no conflict of interest.

Acknowledgments

The authors extend their appreciation to the Deanship of Scientific Research at King Saud University for funding the work through the research group project No. RGP-VPP-120.

References

Ahmad, S.F., Zoheir, K.M., Abdel-Hamied, H.E., Attia, S.M., Ashour, A.E., Bakheet, S.A., Abd-Allah, A.R., 2013. Grape seed proanthocyanidin extract has potent anti-arthritic effects on collagen-induced arthritis by modifying the T cell balance. Int. Immunopharmacol. 17, 79–87.

Ansari, M.A., Maayah, Z.H., Bakheet, S.A., El-Kadi, A.O., Korashy, H.M., 2013. The role of aryl hydrocarbon receptor signaling pathway in cardiotoxicity of acute lead intoxication in vivo and in vitro rat model. Toxicology 306, 40–49.

Ahmad, S.F., Zoheir, K.M., Bakheet, S.A., Ashour, A.E., Attia, S.M., 2014a. Poly(ADP-ribose) polymerase-1 inhibitor modulates T regulatory and IL-17 cells in the prevention of adjuvant induced arthritis in mice model. Cytokine 68, 76–85.

Ahmad, S.F., Zoheir, K.M., Abdel-Hamied, H.E., Alrashidi, I., Attia, S.M., Bakheet, S.A., Ashour, A.E., Abd-Allah, A.R., 2014b. The role of a histamine 4 receptor as an anti-inflammatory target in carrageenan-induced pleurisy in mice. Immunology 142 (3), 374–383.

Ahmad, S.F., Zoheir, K.M., Abdel-Hamied, H.E., Attia, S.M., Bakheet, S.A., Ashour, A.E., Abd-Allah, A.R., 2014c. Grape seed proanthocyanidin extract protects against carrageenan-induced lung inflammation in mice through reduction of pro-inflammatory markers and chemokine expressions. Inflammation 37, 500–511.

Ahmad, S.F., Zoheir, K.M., Abdel-Hamied, H.E., Attia, S.M., Bakheet, S.A., Ashour, A.E., Abd-Allah, A.R., 2014d. Amelioration of autoimmune arthritis by naringin through modulation of T regulatory cells and Th1/Th2 cytokines. Cell. Immunol. 287, 112–120.

Ahmad, S.F., Attia, S.M., Zoheir, K.M., Ashour, A.E., Bakheet, S.A., 2014e. Attenuation of the progression of adjuvant-induced arthritis by 3-aminobenzamide treatment. Int. Immunopharmacol. 19, 52–59.

Ballestas, M.E., Benveniste, E.N., 1995. Interleukin 1-beta- and tumor necrosis factor-alpha-mediated regulation of ICAM-1 gene expression in astrocytes requires protein kinase C activity. Glia 14, 267–278.

Barakat, A., Szick-Miranda, K., Chang, I.F., Guyot, R., Blanc, G., Cooke, R., Delseny, M., Bailey-Serres, J., 2001. The organization of cytoplasmic ribosomal protein genes in the Arabidopsis genome. Plant Physiol. 127, 398–415.

Borish, L.C., Steinke, J.W., 2003. Cytokines and chemokines. J. Allergy Clin. Immunol. 111, 460–475.

Cornelius, L.A., Taylor, J.T., Degitz, K., Li, L.J., Lawley, T.J., Caughman, S.W., 1993. A 5′ portion of the ICAM-1 gene confers tissue-specific differential expression levels and cytokine responsiveness. J. Invest. Dermatol. 100, 753–758.

Cuzzocrea, S., Zingarelli, B., Hake, P., Salzman, A.L., Szabo, C., 1998. Anti-inflammatory effects of mercaptoethylguanidine, a combined inhibitor of nitric oxide synthase and peroxynitrite scavenger, in carrageenan-induced models of inflammation. Free Rad. Biol. Med. 24, 450–459.

Chen, Y., Yang, L., Lee, T.J., 2000. Oroxylin A inhibition of lipopolysaccharide-induced iNOS and COX-2 gene expression via suppression of nuclear factor-kappaB activation. Biochem. Pharmacol. 59, 1445–1457.

Christopherson, K., Hromas, R., 2001. Chemokine regulation of normal and pathologic immune responses. Stem Cells 19, 388–396.

Cuzzocrea, S., Mazzon, E., Dugo, L., Serraino, I., Di Paola, R., Genovese, T., De Sarro, A., Caputi, A.P., 2002. Absence of endogenous interleukin-10 enhances the evolution of acute lung injury. Eur. Cytokine Netw. 13, 285–297.

Cuzzocrea, S., Mazzon, E., Di Paola, R., Genovese, T., Patel, N.S., Muià, C., Threadgill, M.D., De Sarro, A., Thiemermann, C., 2004. 5-Aminoisoquinolinone reduces colon injury by experimental colitis. Naunyn Schmiedebergs Arch. Pharmacol. 370, 464–473.

D'Amours, D., Desnoyers, S., D'Silva, I., Poirier, G.G., 1999. Poly(ADP-ribose) polymerase-1 reactions in the regulation of nuclear functions. Biochem. J. 342, 249–268.

Esposito, E., Cuzzocrea, S., 2009. Superoxide, NO, peroxynitrite and PARP in circulatory shock and inflammation. Front. Biosci. (Landmark Ed.) 14, 263–296.

Farombi, E.O., Shrotriya, S., Surh, Y.-J., 2009. Kolaviron inhibits dimethyl nitrosamine-induced liver injury by suppressing COX-2 and iNOS expression via NF-kB and AP-1. Life Sci. 84, 149–155.

Gao, H., Guo, R.F., Speyer, C.L., Reuben, J., Neff, T.A., Hoesel, L.M., 2004. Stat3 activation in acute lung injury. J. Immunol. 172, 7703–7712.

Gonzalez-Rey, E., Martínez-Romero, R., O'Valle, F., Aguilar-Quesada, R., Conde, C., Delgado, M., Oliver, F.J., 2007. Therapeutic effect of a poly(ADP-ribose) polymerase-1 inhibitor on experimental arthritis by down-regulating inflammation and Th1 response. PLoS ONE 31 (2), e1071.

Hurst, S.D., Muchamuel, T., Gorman, D.M., Gilbert, J.M., Clifford, T., Kwan, S., 2002. New IL-17 family members promote Th1 or Th2 responses in the lung: in vivo function of the novel cytokine IL-25. J. Immunol. 169, 443–453.

Hori, S., Nomura, T., Sakaguchi, S., 2003. Control of regulatory T cell development by the transcription factor Foxp3. Science 299, 1057–1061.

Hakme, A., Wong, H.K., Dantzer, F., Schreiber, V., 2008. The expanding field of poly(ADPribosyl) action reactions. EMBO Rep. 9, 1094–1100.

Hendryk, S., Czuba, Z.P., Jedrzejowska-Szypulka, H., Szliszka, E., Phillips, V.A., Threadgill, M.D., 2008. Influence of 5-aminoisoquinolin-1-one (5-AIQ) on neutrophil chemiluminescence in rats with transient and prolonged focal cerebral ischemia and after reperfusion. J. Physiol. Pharmacol. 59, 811–822.

Hesslinger, C., Strub, A., Boer, R., Ulrich, W.R., Lehner, M.D., Braun, C., 2009. Inhibition of inducible nitric oxide synthase in respiratory diseases. Biochem. Soc. Trans. 37, 886–891.

Impellizzeri, D., Esposito, E., Mazzon, E., Paterniti, I., Di Paola, R., Bramanti, P., Cuzzocrea, S., 2011. Effect of apocynin, a NADPH oxidase inhibitor, on acute lung inflammation. Biochem. Pharmacol. 1, 636–648.

Karin., M., Delhase, M., 1998. JNK or IKK, AP-1 or NF-kappaB, which are the targets for MEK kinase 1 action? Proc. Natl. Acad. Sci. U.S.A. 95, 9067–9069.

Katz, Y., Nadiv, O., Beer, Y., 2001. Interleukin-17 enhances tumor necrosis factor alpha-induced synthesis of interleukin 1, 6, and 8 in skin and synovial fibroblasts: a possible role as a fine tuning cytokine in inflammation processes. Arthritis Rheum. 44, 2176–2184.

Ko, K., Yamazaki, S., Nakamura, K., Nishioka, T., Hirota, K., Yamaguchi, T., Shimizu, J., Nomura, T., Chiba, T., Sakaguchi, S., 2005. Treatment of advanced tumors with agonistic anti-GITR mAb and its effects on tumor-infiltrating Foxp3CD25CD4 regulatory T cells. J. Exp. Med. 202, 885–891.

Kirchberger, S., Vetr, H., Majdic, O., Stockinger, H., Stockl, J., 2006. Engagement of ICAM-1 by major group rhinoviruses activates the LFA-1/ICAM-3 cell adhesion pathway in mononuclear phagocytes. Immunobiology 211, 537–547.

Kraus, W.L., 2008. Transcriptional control by PARP-1: chromatin modulation, enhancer-binding, coregulation, and insulation. Curr. Opin. Cell Biol. 202, 294–302.

Kane, A., Deenick, E.K., Ma, C.S., Cook, M.C., Uzel, G., Tangye, S.G., 2014. STAT3 is a central regulator of lymphocyte differentiation and function. Curr. Opin. Immunol. 28C, 49–57.

Lewinsohn, D.M., Bargatze, R.F., Butcher, E.C., 1987. Leukocyte-endothelial cell recognition: evidence of a common molecular mechanism shared by neutrophils, lymphocytes, and other leukocytes. J. Immunol. 138, 4313–4321.

Levy, D.E., Lee, C.K., 2002. What does STAT-3 do? J. Clin. Invest. 109, 1143–1148.

Lina, Q., Jin, L., Caob, Z., Li, H., Xua, Y., 2008. Protective effect of *Acanthopanax senticosus* extract against endotoxic shock in mice. J. Ethnopharmacol. 118, 495–502.

May, C., Williams, O., Milner, A.D., Peacock, J., Rafferty, G.F., Hannam, S., Greenough, A., 2009. Relation of exhaled nitric oxide levels to development of bronchopulmonary dysplasia. Arch. Dis. Child Fetal Neonatal Ed. 94, F205–F209.

Moon, D.O., Kim, M.O., Kang, S.H., 2009. Sulforaphane suppresses TNF-α-mediated activation of NF-kB and induces apoptosis through activation of reactive oxygen species-dependent caspase-3. Cancer Lett. 274, 132–142.

Nishibori, M., Takahashi, H.K., Mori, S., 2003. The regulation of ICAM-1 and LFA-1 interaction by autacoids and statins: a novel strategy for controlling inflammation and immune responses. J. Pharmacol. Sci. 92, 7–12.

Nocentini, G., Riccardi, C., 2005. GITR: a multifaceted regulator of immunity belonging to the tumor necrosis factor receptor superfamily. Eur. J. Immunol. 35, 1016–1022.
Nicolescu, A.C., Holt, A., Kandasamy, A.D., Pacher, P., Schulz, R., 2009. Inhibition of matrix metalloproteinase-2 by PARP inhibitors. Biochem. Biophys. Res. Commun. 387, 646–650.
Olabisi, O.A., Soto-Nieves, N., Nieves, E., Yang, T.T., Yang, X., Yu, R.Y., Suk, H.Y., Macian, F., Chow, C.W., 2008. Regulation of transcription factor NFAT by ADP-ribosylation. Mol. Cell Biol. 28 (9), 2860–2871.
Oliveira, S.H.P., Canetti, C., Ribeiro, R.A., Cunha, F.Q., 2008. Neutrophil migration induced by IL-1β depends upon LTB4 released by macrophages and upon TNF-α and IL-1β released by mast cells. Inflammation 31, 36–46.
Pfitzner, E., Kliem, S., Baus, D., Litterst, C.M., 2004. The role of STATs in inflammation and inflammatory diseases. Curr. Pharm. Des. 10, 2839–2850.
Di Paola, R., Mazzon, E., Muia, C., Terrana, D., Greco, S., Britti, D., Santori, D., Oteri, G., Cordasco, G., Cuzzocrea, S., 2007. 5-Aminoisoquinolin-1(2*H*)-one, a water-soluble poly (ADP-ribose) polymerase (PARP) inhibitor reduces the evolution of experimental periodontitis in rats. J. Clin. Periodontol. 34, 95–102.
Pacher, P., Szabo, C., 2007. Role of poly(ADP-ribose) polymerase-1 (PARP-1) in cardiovascular diseases: the therapeutic potential of PARP inhibitors. Cardiovasc. Drug Rev. 25, 235–260.
Paul, E.L., Lunardelli, A., Caberlon, E., Oliveira, C.B., Santos, R.C.V., Biolchi, V., Bastos, C.M.A., Moreira, K.B., Nunes, F.B., Gosmann, G., Oliveira, J.R., 2009. Anti-inflammatory and immunomodulatory effects of *Baccharis trimera* aqueous extract on induced pleurisy in rats and lymphoproliferation in vitro. Inflammation 32, 419–425.
Renner, E.D., Rylaarsdam, S., Anover-Sombke, S., Rack, A.L., Reichenbach, J., Carey, J.C., Zhu, Q., Jansson, A.F., Barboza, J., Schimke, L.F., 2008. Novel signal transducer and activator of transcription 3 (STAT3) mutations, reduced T(H)17 cell numbers, and variably defective STAT3 phosphorylation in hyper-IgE syndrome. J. Allergy Clin. Immunol. 122, 181–187.
Sambrook, J., Fritsch, E.F., Maniatatis, T., Ford, N. (Eds.), 1989. Molecular Cloning. A Laboratory Manual. Cold Spring Harbour Laboratory Press, Plainview, NY.
Seder, R.A., Paul, W.E., Davis, M.M., Fazekas, de St., Groth, B., 1992. The presence of interleukin 4 during in vitro priming determines the lymphokine-producing potential of CD4CT cells from T cell receptor transgenic mice. J. Exp. Med. 176, 1091–1098.
Sakaguchi, S., Sakaguchi, N., Asano, M., Itoh, M., Toda, M., 1995. Immunologic tolerance maintained by activated T cells expressing IL-2 receptor α-chains (CD25): breakdown of a single mechanism of self-tolerance causes various autoimmune diseases. J. Immunol. 155, 1151–1164.
Shall, S., De Murcia, G., 2000. Poly(ADP-ribose) polymerase-1: what have we learned from the deficient mouse model? Mutat. Res. 460, 1–15.
Szabo, G., Bahrle, S., Stumpf, N., 2002. Poly(ADP-ribose) polymerase inhibition reduces reperfusion injury after heart transplantation. Circ. Res. 90, 100–106.
Szabo, C., 2006. Poly(ADP-ribose) polymerase activation by reactive nitrogen species-relevance for the pathogenesis of inflammation. Nitric Oxide 141, 69–79.
Schymeinsky, J., Mócsai, A., Walzog, B., 2007. Neutrophil activation via beta(2) integrins (CD11/CD18): molecular mechanisms and clinical implications. Thromb. Haemost. 98, 262–273.
Saenz, L., Lozano, J.J., Valdor, R., Baroja-Mazo, A., Ramirez, P., Parrilla, P., Aparicio, P., Sumoy, L., Yélamos, J., 2008. Transcriptional regulation by poly(ADP-ribose) polymerase-1 during T cell activation. BMC Genomics 16 (9), 171.
Seevaratnam, R., Patel, B.P., Hamadeh, M.J., 2009. Comparison of total protein concentration in skeletal muscle as measured by the Bradford and Lowry assays. J. Biochem. 145, 791–797.
Sun, S.X., Li, Y.M., Fang, W.R., Cheng, P., 2010. Effect and mechanism of AR-6 in experimental rheumatoid arthritis. Clin. Exp. Med. 10 (2), 113–121.
Tamura, D.Y., Moore, E.E., Johnson, J.L., Zallen, G., Aiboshi, J., Silliman, C.C., 1998. p38 mitogen-activated protein kinase inhibition attenuates intercellular adhesion molecule-1 up-regulation on human pulmonary microvascular endothelial cells. Surgery 124, 403–407.
Virag, L., Szabo, C., 2002. The therapeutic potential of poly(ADP-ribose) polymerase inhibitors. Pharmacol. Rev. 54, 375–429.
Zingarelli, B., Salzman, A.L., Szabo, C., 1998. Genetic disruption of poly (ADP-ribose) synthetase inhibits the expression of *P*-selectin and intercellular adhesion molecule-1 in myocardial ischemia/reperfusion injury. Circ. Res. 83, 85–94.
Zhou, H.Y., Shin, E.M., Guo, L.Y., 2008. Anti-inflammatory activity of 4-methoxyhonokiol is a function of the inhibition of iNOS and COX-2 expression in RAW 264.7 macrophages via NF-kB JNK and p38 MAPK inactivation. Eur. J. Pharmacol. 586, 340–349.